Stimulated Brillouin Cavity Optomechanics in Liquid Droplets

A. Giorgini,[1] S. Avino,[1] P. Malara,[1] P. De Natale,[2] M. Yannai,[3] T. Carmon,[3] and G. Gagliardi[1,*]

[1]*Consiglio Nazionale delle Ricerche, Istituto Nazionale di Ottica (INO), via Campi Flegrei,*
34—Comprensorio A. Olivetti, 80078 Pozzuoli (Naples), Italy
[2]*Consiglio Nazionale delle Ricerche, Istituto Nazionale di Ottica (INO), Largo E. Fermi 6, 50125 Firenze, Italy*
[3]*Mechanical Engineering Department, Technion Israel Institute of Technology, 32000 Haifa, Israel*

Liquid droplets are ubiquitous in nature wherein surface tension shapes them into perfect spheres with atomic-scale smooth surfaces. Here, we use stable droplets that cohost equatorial acoustical and optical resonances phase matched to enable the exchange of energy and momentum between sound and light. Relying on free-space laser excitation of multiple whispering-gallery modes, we harness a triple-resonant forward Brillouin scattering to stimulate optomechanical surface waves. Nonlinear amplification of droplet vibrations in the 60–70 MHz range is realized with spectral narrowing beyond the limit of material loss, thereby activating the droplet as hypersound-laser emitter.

The interaction of electromagnetic radiation and mechanical motion via ponderomotive forces has been extensively investigated in solid optical microresonators. Most of these experiments rest on the parametric excitation of vibrations in various structures, such as suspended-mirror microcavities, microtoroids, microspheres, nanorods, etc., using radiation pressure as a coupling mechanism [1]. An alternative way of exciting mechanical vibrations with electromagnetic radiation is inelastic light scattering by a traveling sound wave [2]. Light-sound interactions were first suggested by Brillouin in 1922 [3] and later served in lasers using the mechanism generally referred to as stimulated Brillouin scattering (SBS) [4]. Basically, SBS in dielectrics can be driven by the refractive-index modulation induced in the material by the light field itself. Following the interaction with an acoustic wavefront, moving away from or towards the incident optical wave, the frequency of the scattered light is shifted downward [5–7] or upward [8] thereby generating a Stokes or an anti-Stokes sideband, respectively. The beating between the laser and Stokes fields contains a component at their difference frequency, i.e., at the sound frequency. The material response to this interference, via electrostriction or absorption, may in turn drive a sound wave that reinforces the Stokes wave, and so forth. If energy and momentum are conserved, this positive feedback becomes self-sustained and leads to an exponential growth of the Stokes amplitude. If this process occurs in a high optical quality (Q) whispering-gallery-mode (WGM) microresonator, with resonant pump, Stokes and acoustic waves, the result is a significant amplification of the vibrations with energy transfer from the radiation to the mechanical oscillator [6–8]. Momentum conservation (phase matching) also suggests that a reversal of the scattering direction from backward to forward allows accessing

vibrations rates on the order of 50–100 MHz [7], much lower than the typical Brillouin values ($\sim$GHz), which would provide the benefit of a strongly reduced material dissipation for generation of intense hypersonic waves [2]. Nonetheless, satisfying phase matching may be challenging in forward scattering due to the requirement of having two neighboring WGMs with propagation constants differing by the phonon momentum.

About three decades ago, pioneering works [9] with high-intensity pulsed lasers and theoretical models [10] investigated the generation of backward SBS in falling micrometer-sized droplets fabricated by aerosol generators. However, no attempt of observing forward SBS and no Brillouin optomechanics experiment with continuous-wave lasers in liquid droplets have been reported to date. In this Letter, we experimentally demonstrate optical amplification of hypersonic waves circumferentially resonating in a stable droplet. Here, we harness coresonating acoustic and electromagnetic whispering-gallery modes that interact to exchange energy and momentum within the liquid cavity via stimulated Brillouin scattering, thus enabling an optofluidic hypersound laser.

Our microcavity is a 140-μm-radius (R) droplet made from a low-viscosity liquid polymer [Fig. 1(a)]. The microresonators are fabricated by immersion of a bare silica optical fiber in a pure sample of Xiameter® PMX-200 silicone oil (50-cSt kinematic viscosity): in this way, small droplets, with diameters ranging from 100 to 1000 μm, form spontaneously at the fiber tip due to surface tension and remain stably suspended along the vertical direction thanks to solid-liquid adhesion forces. The excitation and interrogation light source is a temperature-stabilized diode laser emitting around a wavelength of 640 nm. High-quality whispering-gallery modes are excited by
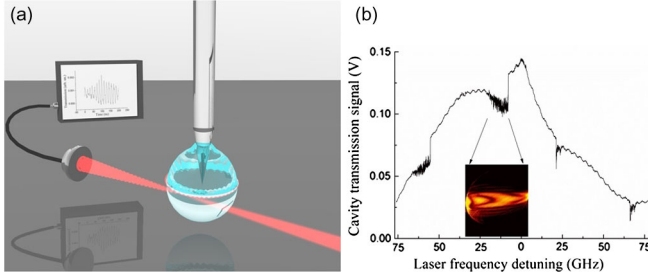
FIG. 1. (a) Pictorial view of the optical setup. A high-Q optical microresonator is obtained suspending a silicone-oil droplet by the tip of a silica holder (not to scale). A red laser beam is focused tangentially to the droplet rim to excite optical and acoustic WGMs. The generated vibration propagates along an equatorial trajectory and scatters (Brillouin) the incident light. A time-domain oscillation (~14-ns period) on the transmitted power, resulting from the beat between the laser and Stokes fields, is shown as an example by the monitor screen. (b) Optical resonances are shown as observed on the transmission of a 140-μm-radius droplet along an ascending and descending wavelength scan, from left to right, respectively. Fast amplitude oscillations and thermal broadening effects are visible on each resonance. Inset: Camera view of the out-scattered radiation when the laser is resonant with the strongest mode.

focusing its free-space beam tangential to the droplet surface without using any coupling device [11]. For this purpose, a piezoactuated three-axes translation stage is used for careful alignment of the droplet into the beam. A complete description of the experimental setup can be found in Refs. [12,13]. The optical power effectively coupled to the cavity mode in our Brillouin optomechanics experiments is measured to be approximately 6% of the incident power (the latter ranging from 1 to 8 mW). The beam transmitted just after the droplet is detected by a fast photodetector (10-GHz electrical bandwidth) to interrogate optical and acoustic resonances.

Let us consider a pump optical wave at frequency f_l and a traveling (spontaneous) acoustic wave resonantly propagating along the droplet equator at a frequency f_a that satisfies the equation

$$2\pi R = m_a V/f_a, \tag{1}$$

where V is the sound velocity in the liquid and m_a is an integer representing the number of acoustic wavelengths along the circumference. This mechanical mode creates an optical grating that photoelastically scatters the pump beam: since the mechanical wave recedes with velocity V, it Doppler redshifts the scattered light generating a Stokes wave at frequency

$$f_s = f_l - f_a. \tag{2}$$

If the Stokes frequency falls into a second WGM resonance, its beat with the pump can in turn excite a vibration at f_a by electrostriction. If this optically induced

mechanical modulation also travels at the speed of sound, the whole process becomes self-sustained. The Stokes wave then undergoes a significant amplification that may lead to a Brillouin laser. This phenomenological description can be formalized by imposing energy and momentum conservation in the coupled-wave equation for the mechanical and optical waves [7]. Its solution reveals that in this process the propagation constant of the pump β_l must equal the sum of the propagation constants of the Stokes and acoustic modes β_s and β_a, respectively:

$$\beta_l = \beta_s + \beta_a. \tag{3}$$

SBS in high-Q microresonators is thus possible only when a triply resonant condition is satisfied within the cavity for the pump, Stokes, and acoustic waves. This task can be accomplished in multiple-mode resonators if the intermodal distance matches the pump-Stokes energy difference, which is made easier by the ability to change the optical-mode spatial distribution and transverse order [7,14]. Actually, phase matching may be achieved as well if the pump photons and the scattered photons both populate the same optical resonance to a good extent [5,10]. For silicone-oil droplets, this is feasible since the absorption-limited Q factor ranges from 10^6 to 10^7; i.e., the resonances have linewidths of 50–500 MHz [13], where WGMs with different azimuthal and radial orders may coexist. Their simultaneous excitation is facilitated by the free-space illumination scheme [Fig. 1(a)] [11,15]. Coupling to the microcavity relies on surface scattering that provides ample margins to control the WGMs' spatial configuration through droplet alignment. On the other hand, from momentum conservation, two interacting WGMs must exhibit azimuthal mode numbers satisfying Eq. (3); i.e. $m_s - m_l = m_a$, where m_a is given by Eq. (1).

Expressing Eq. (3) in terms of the WGM wave numbers for a spherical microresonator [14],

$$\beta_{m_k q_k} \cong \frac{1}{R}\left[m_k + \alpha_{q_k}\left(\frac{m_k}{2}\right)^{1/3} - \frac{1}{n\sqrt{n^2 - 1}}\right], \tag{4}$$

where n is the silicone-oil refractive index and α_{q_k} is the qth zero of the Airy function [Ai$(-\alpha_q)$] for the kth mode ($k = l, s$), and inserting the acoustic angular momentum number $m_a = 2\pi f_a R/\lambda$, one obtains for the condition on the azimuthal quantum numbers

$$\frac{2\pi f_a R}{V} \cong \left[\left(\frac{m_s}{2}\right)^{1/3}(\alpha_{q_s} - \alpha_{q_l})\right], \tag{5}$$

where $n \approx 1.4$, $R = 140$ μm, $V \approx 1350$ m/s, using the approximation $m_s \cong m_l$. For example, considering a resonant acoustic mode with $f_a = 70$ MHz, from Eq. (1) the angular momentum number turns out to be $m_a \approx 45$.
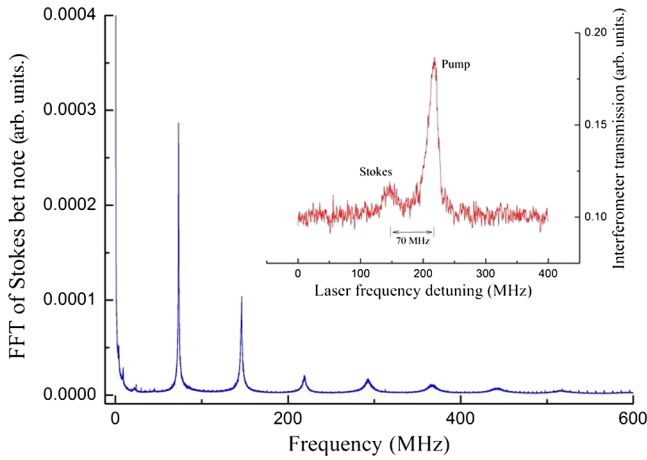
FIG. 2. FFT of the droplet transmission signal. The Fourier spectrum shows several oscillations with the largest peaks from 70 to 500 MHz (pump power of 360 μW). The inset shows a Fabry-Pèrot spectral analysis of the microcavity transmitted light (maximum pump power) that points out the generation of a new optical field due to (Stokes) forward SBS.

Substituting the above values in Eq. (5) and considering that $m_s \cong m_l = 2\pi R n/\lambda \cong 1924$, we obtain that this particular acoustic wave would be phase matched with optical waves having radial numbers $q_l = 1$ and $q_s = 4$, that resonantly propagate in the droplet with azimuthal numbers m_l and $m_s = m_l - m_a = m_l - 45$. This suggests that the coupling between the two neighboring optical modes can be optimized acting on their radial orders.

In order to interrogate the droplet oscillator, the laser is wavelength swept to observe optical WGMs on the directly transmitted beam [Fig. 1(a)]. When the equator length is an integer multiple of the wavelength, a WGM is excited and a fraction of the incident power is coupled to circumferentially resonate into it. As shown in Fig. 1(b), sharp dips appear on the microcavity transmission while the laser is scanned through a WGM with decreasing wavelength (increasing frequency). On the backward scan, instead, it is worth noting the strongly broadened and asymmetric resonance line shapes due to thermally induced nonlinearities [13] caused by the intracavity power buildup. This effect drives a self-locking mechanism that maintains the laser in the vicinity of the resonance without using any active optoelectronic feedback [16]. In the inset of Fig. 1(b), a camera recording of the out-scattered radiation when the laser is thermally self-locked to a strong WGM is shown: the deep intensity modulation indicates the presence of different equatorial resonances associated, as expected, with WGMs of different orders [17]. In this condition, the resonant transmitted power exhibits strong amplitude oscillations, in the MHz range, which cannot be interpreted by the occurrence of droplet bulk acoustic modes [18]. Figure 2 shows the FFT of the transmission signal between 60 and 300 MHz. The spectrum contains distinct sharp features at 69.5 ± 0.8, 140 ± 3, and 210 ± 10 MHz that are believed to originate from the beats between the pump laser and Brillouin scattered modes. The numerically simulated spatial distributions of the perturbation for three different surface acoustic modes [19]
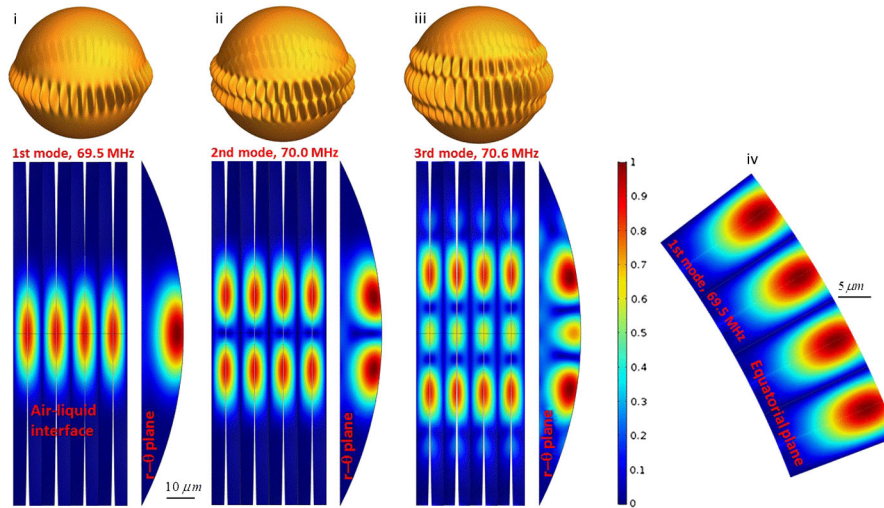

FIG. 3. Acoustic mode FEM simulation. Different longitudinal modes resonating along the circumference with an azimuthal mode number $m = 45$ are numerically analyzed and plotted along with their resonance frequencies. (i)–(iii) Top: Three acoustic modes in ascending transverse order are shown in a 3D artistic illustration with purposely exaggerated modulation depth. (i)–(iii) Bottom: The three modes are shown with their absolute displacement fields (see scale on color bar): left, at the liquid-phase boundary ($\theta - \varphi$ plane); right, at the radial-polar plane ($r - \theta$). (iv) The first mode seen at the equatorial plane ($r - \varphi$). The FEM simulation is carried out with COMSOL MULTIPHYSICS® for silicone-oil droplets, using Young's modulus $E = 1.641$ GPa, density $\rho = 971$ kg/m^3, Poisson's ratio $\nu = 0.17$, and cavity radius $R = 140$ μm. The model considers an azimuthal slice of the droplet corresponding to one quarter wavelength of the acoustic mode.
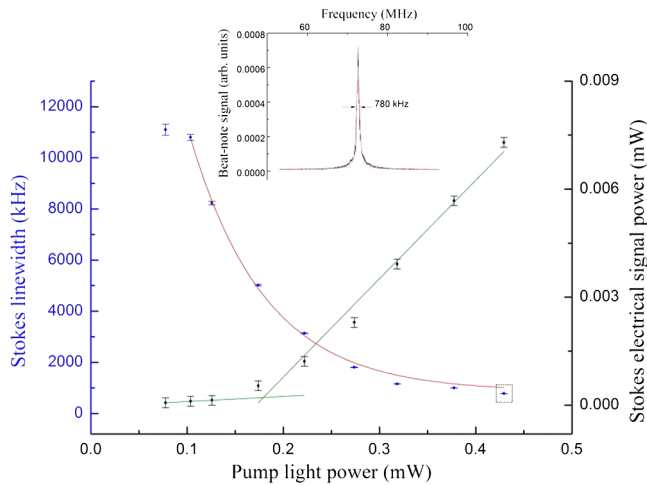
FIG. 4. Stokes linewidth and power versus pump light power coupled to the droplet. The Stokes beat-note power (black squares) increases with pump and exhibits a knee with slope change at a threshold power of ∼180 μW (error bars are statistical uncertainties from Lorentzian fits). The beat-note linewidth (blue points) narrows exponentially with increasing power from an initial value of 11.1 ± 0.2 MHz (35% wider than the value expected from the intrinsic material loss; see ref. [21]) down to 780 ± 4 kHz at the maximum power level (dotted square on the graph). The narrowest observed line shape is shown in the inset with a red line representing a Lorentzian fit.

of a 140-μm oil droplet are shown in Fig. 3, pointing out a resonance around 70 MHz. These values are in good agreement with the first peak shown in Fig. 2, thus confirming that the experimentally observed feature is due to cavity-enhanced forward SBS by an acoustic mode of whispering-gallery type. The higher harmonics at 140 and 210 MHz may result from cascaded Brillouin processes, i.e., scattering induced by the first Stokes lines and subsequent four-wave mixing [20]. Subsequently, we analyzed the transmitted cavity light with a scanning Fabry-Pèrot interferometer when the laser was on resonance. In the inset of Fig. 2, the Fabry-Pèrot transmission shows a sideband oscillating at a frequency red detuned by 70 MHz from the pump frequency, which confirms the presence of the new optical component associated with the Stokes field.

Figure 4 illustrates how the intracavity stimulated SBS process enhances a droplet surface wave and increases its quality factor. The beat-note power grows exponentially with increasing pump with a threshold level around 180 μW. This is the point where a transition occurs between an initial condition in which Brownian fluctuations dominate and a new regime whereby the vibration mode is optically excited until the Brillouin gain provides acoustical amplification and eventually becomes larger than the material loss. Indeed, the beat-note linewidth drops from a starting value of ∼11 MHz, corresponding to the intrinsic mechanical quality factor $Q_a = 5$ [21],

down to ∼0.8 MHz at maximum power, which corresponds to an effective mechanical quality factor $Q_a^* = 90$.

In conclusion, light stimulated Brillouin optomechanics has been performed in a stable liquid droplet. By virtue of a phase-matched triply resonant interaction between optical and acoustic whispering-gallery modes, a forward-scattering process is allowed that generates surface-acoustic waves at rates much lower than that of typical Brillouin phenomena, thus leading to mechanical finesse near the material limit. Uniquely, we show experimentally that the intracavity enhancement narrows the mechanical feature even further and transforms the droplet into a high-quality optofluidic hypersound laser. Our results can have a significant impact in different fields: in fundamental physics, for studies on viscoelasticity and surface phenomena, as well as in spectroscopy and applications to nonlinear optofluidics and ultrasound-hypersound sensing of materials in liquid phase.

*gianluca.gagliardi@ino.it

[1] M. Asplemeyer, T. J. Kippenberg, and F. Marquardt, Rev. Mod. Phys. **86,** 1391 (2014).

[2] R. Boyd, *Nonlinear Optics* 3rd ed. (Academic Press, New York, 2008).

[3] L. Brillouin, Ann. Phys. (Berlin) **9,** 88 (1922).

[4] N. Bloembergen and Y. R. Shen, Phys. Rev. Lett. **12,** 504 (1964).

[5] I. S. Grudinin, A. B. Matsko, and L. Maleki, Phys. Rev. Lett. **102,** 043902 (2009).

[6] M. Tomes and T. Carmon, Phys. Rev. Lett. **102,** 113601 (2009).

[7] G. Bahl, J. Zehnpfennig, M. Tomes, and T. Carmon, Nat. Commun. **2,** 403 (2011).

[8] G. Bahl, M. Tomes, F. Marquardt, and T. Carmon, Nat. Phys. **8,** 203 (2012).

[9] J.-Z. Zhang and R. K. Chang, J. Opt. Soc. Am. B **6,** 151 (1989).

[10] P. T. Leung and K. Young, Phys. Rev. A **44,** 593 (1991).

[11] A. Ashkin and J. M. Dziedzic, Phys. Rev. Lett. **38,** 1351 (1977).

[12] S. Avino, A. Krause, R. Zullo, A. Giorgini, P. Malara, P. De Natale, H.-P. Loock, and G. Gagliardi, Adv. Opt. Mater. **2,** 1155 (2014).

[13] A. Giorgini, S. Avino, P. Malara, P. De Natale, and G. Gagliardi, Sci. Rep. **7,** 41997 (2017).

[14] A. B. Matsko, A. A. Savchenkov, V. S. Ilchenko, D. Seidel, and L. Maleki, Phys. Rev. Lett. **103,** 257403 (2009).

[15] R. Zullo, A. Giorgini, S. Avino, P. Malara, P. De Natale, and G. Gagliardi, Opt. Lett. **41,** 650 (2016).

[16] T. G. McRae, K. H. Lee, M. McGovern, D. Gwyther, and W. P. Bowen, Opt. Express **17,** 21977 (2009).

[17] A. A. Savchenkov, A. B. Matsko, V. S. Ilchenko, D. Strekalov, and L. Maleki, Phys. Rev. A **76**, 023816 (2007).

[18] R. Dahan, L. L. Martin, and T. Carmon, Optica **3**, 175 (2016).

[19] J. Zehnpfennig, G. Bahl, M. Tomes, and T. Carmon, Opt. Express **19**, 14240 (2011).

[20] G. Lin and Y. K. Chembo, Int. J. Optomechatronics **10**, 32 (2016).

[21] The droplet mechanical quality factor $Q_a = f_a/\Gamma_B$ for the acoustic resonance at $f_a = 69.5$ MHz can be calculated via the acoustical attenuation factor from the dynamic-viscosity coefficient $(\eta = 0.048 \text{ N s/m}^2)$, mass density $(\rho = 960 \text{ kg/m}^3)$, and sound speed (1350 m/s) of silicone oil, which provide a Brillouin linewidth $\Gamma_B = (4\eta/3\rho)(\Omega^2/V^2) \cong 7$ MHz, with $\Omega \equiv 2\pi f_a$. This theoretical estimate differs by 35% from the measured value.